ELSEVIER

Atmospheric Research 59–60 (2001) 199–215

ATMOSPHERIC RESEARCH

www.elsevier.com/locate/atmos

Investigating the small-scale structure of clouds using the δ-correlated closure: effect of particle inertia, condensation/evaporation and intermittency

Christopher A. Jeffery *

Atmospheric Sciences Programme, University of British Columbia, c/o #217 Geography, 1984 West Mall, UBC, Vancouver, BC Canada, V6T 1Z2

Accepted 23 July 2001

Abstract

Equations for the first and second moments of particle density are closed exactly in the large Prandtl number limit, using the δ-correlated closure whereby the turbulent velocity field is assumed to rapidly decorrelate in time. Results are summarized from two recent studies that have investigated the effect of both particle inertia and condensation/evaporation on the viscous–convective subrange. Analytic expressions for the spectrum of inertial particles are presented which show that clumping (preferential concentration) does not occur for Stokes number (*St*) less than about 0.2. Also presented are analytic expressions for the scalar spectrum of cloud liquid water density derived from a simple mean-field model of condensation/evaporation. The model reproduces new experimental observations [J. Geophys. Res. 104 (1999) 6123] of cloud liquid water content (LWC) fluctuations that exhibit anomalous near-inertial scaling. For the first time, the effect of high Reynolds number (Re_λ) velocity field intermittency on preferential concentration is considered in a quantitative manner. A Re_λ-dependent effective Stokes number (St_{eff}) is derived that is proportional to the square root of the flatness factor of the longitudinal velocity derivative. In the atmospheric boundary-layer, $St_{eff} \approx 2.7\ St$. These results support Shaw et al.'s [J. Atmos. Sci. 55 (1998) 1965] hypothesis that velocity field intermittency tends to increase preferential concentration at $St < 1$. However, in contrast with Shaw et al., I demonstrate that, in real turbulence, vortex tubes do not statistically affect St_{eff} and, hence, preferential concentration.

Keywords: Intermittency; Preferential concentration; Stokes number; Kraichnan model; Cloud droplet spectra; Condensational growth

* Los Alamos National Laboratory (NIS-2), PO Box 1663, Mail Stop C-323, Los Alamos, NM 87545, USA. Tel.: +1-505-667-4105; fax: +1-505-667-9208.

E-mail address: cjeffery@lanl.gov (C.A. Jeffery).

PII: S0169-8095(01)00116-8

1. Introduction

Recently, both Pinsky and Khain (1997) and Shaw et al. (1998) have considered the effect of cloud droplet inertia on the droplet size distribution during condensational growth. Despite the commonality of the phenomena investigated, their conclusions are remarkably different. Pinsky and Khain (1997) suggest that droplet inertia results in "inertial drop mixing," whereby two small neighboring volumes of air exchange drops according to the inertia-induced velocity divergence of the droplets. As a result, two volumes with greatly differing size distributions at cloud base become homogenized as the volumes are lifted adiabatically, while two volumes that are identical at the cloud base will remain homogenized but will be stochastically different at the cloud top. Results from a more refined model of inertial drop mixing are discussed in detail in Pinsky et al. (1999).

The Shaw et al. (1998) hypothesis, on the other hand, is distinctly different and much bolder. In their model of inertial effects, vortex tubes and thus the intermittency of large Reynolds number (Re_λ) atmospheric flows plays a central role. Although a velocity intermittency effect had been hypothesized earlier (Tennekes and Woods, 1973; Cooper and Baumgardner, 1989), in the Shaw model, the geometry of the fine-scale structure plays a key role for the first time. Shaw et al. (1998) argue that cloud droplets accumulate in regions of high strain and low vorticity in a turbulent flow due to inertia—a phenomena known as "preferential concentration." In contrast to Pinsky and Khain's (1997) inertial mixing, they further suggest that a non-uniform droplet field implies a non-uniform supersaturation field, which leads to a broader distribution of droplet growth rates. However, a broad distribution of growth rates will impact the size distribution only if the growth rate renewal time is very long, $\mathcal{O}(10\ \mathrm{s})$. Thus, Shaw et al. (1998) make one further assumption: vortex tubes with lifetimes $\tau_s = \mathcal{O}(10\ \mathrm{s})$ at large Re_λ trap droplets in a relatively high supersaturation environment for an eddy-trapping time $\tau_T \approx \tau_s$. Thus, we have the Shaw model of "inertial drop trapping" in contradistinction to Pinsky and Khain's (1997) inertial drop mixing.

In a short comment, Grabowski and Vaillancourt (1999) question a number of Shaw et al.'s (1998) assumptions. In particular, Grabowski and Vaillancourt (1999) suggest that (i) droplet sedimentation, not considered by Shaw et al. (1998), substantially decreases τ_T; (ii) the volume fraction of vortex tubes is too small to account for an appreciable vortex trapping mechanism; and (iii) the Stokes number (St)—the ratio between the particle response time due to its inertia and the Eulerian turbulence time-scale—is too small for significant preferential concentration to occur. They estimate that for typical atmospheric conditions and growing droplets (radius $r \leq 15\ \mu\mathrm{m}$) $St \leq 0.07$, whereas laboratory experiments demonstrate that significant preferential concentration occurs for $St = \mathcal{O}(1)$.

In response to (iii), Shaw et al. (1999) argue that at high Reynolds numbers where intense vortex tubes are present, the Stokes number range for preferential concentration increases significantly. Support for this argument comes from direct numerical simulation (DNS) experiments at fixed St (Reade and Collins, 2000; Wang et al., 2000) that demonstrate an increase in particle clumping with increasing Reynolds number.

Adding fuel to this debate, Davis et al. (1999) present horizontal spectra $\phi(k_x)$ of cloud liquid water content (q_l), measured at an unprecedented resolution of 4 cm during the first winter Southern Ocean Cloud Experiment (SOCEX I), that exhibit an anomalously large variance at small-scales. The scalar spectrum from the ensemble-average of the flight segments is shown in Fig. 1 (□), along with the normal inertial-convective and viscous–convective regimes (—). What is particularly intriguing about these new observations is the implication for the scalar dissipation rate χ; with the new scale break, χ in the viscous–convective regime is a factor of 20 larger than the inertial–convective χ; suggesting that a source of scalar variance is present on scales of tens of centimeters. Marshak et al. (1998) suggest that the strong variability shown in Fig. 1 on scales of 4 cm to 4 m is consistent with Shaw et al.'s (1998) discussion of strong preferential concentration, while Mazin (1999) proposes that the non-inertial–convective scaling is caused by the temporal relaxation of the supersaturation to its steady state value.

In this article, I summarize recent investigations of the effect of both particle inertia (Jeffery, 2000, 2001b) and condensation/evaporation (Jeffery, 2001a) on the small-scale variability of cloud droplets, and I present new results on high Re_λ droplet clumping. These studies exploit the availability of an exact closure of the advection–diffusion equation for large particles at small scales discussed in Section 2. In Section 3, I present an analytic expression for the scalar spectrum of inertial particles valid in the small St regime

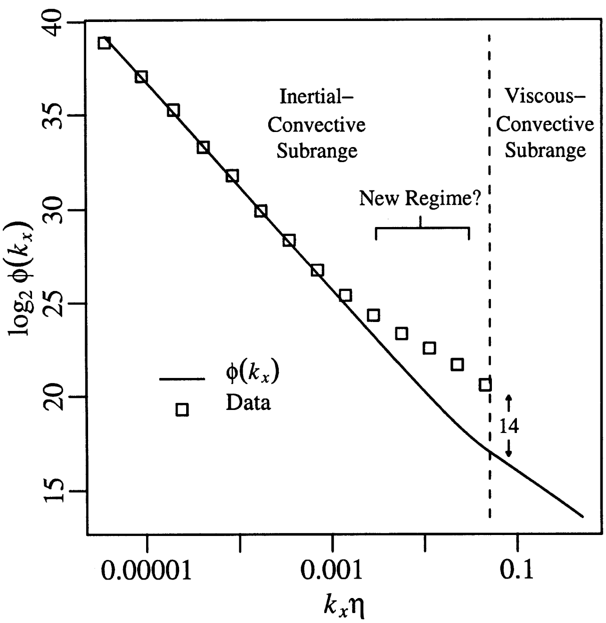

Fig. 1. Ensemble-averaged 1D scalar spectrum for cloud q_l data measured during the SOCEX field program and first presented in Marshak et al. (1998). A typical atmospheric value of 0.76 mm is assumed for the Kolmogorov length η. Also shown is the usual 1D inertial–convective/viscous–convective scaling. The observed spectrum is a factor of 20 greater than the normal spectrum in the viscous–convective regime.

($St < 1$), and in Section 4, a model of anomalous small-scale variability in condensation clouds is introduced. In Section 5, I derive new results concerning the effect of velocity field intermittency on preferential concentration. An effective Stokes number is determined that is an explicit function of the Taylor microscale Reynolds number of the flow. The impact of velocity field intermittency on the preferential concentration of atmospheric cloud droplets is assessed. In Section 6, Shaw et al.'s (1999) hypothesis that vortex tubes significantly increase the Stokes number range for preferential concentration is examined, and in Section 7, the effect of velocity field intermittency on sedimentation rates is discussed. Section 8 is reserved for conclusions.

2. δ-Correlated closure

Numerical and theoretical studies (Kraichnan, 1968; Jeffery, 2000 and references therein) have shown that the δ-correlated closure is an exact closure for the advection–diffusion equation in the small-scale, large Prandtl number limit. The δ-correlated model derives its name from the temporal properties of the velocity field which are assumed to rapidly decorrelate. The key simplification afforded by the δ-correlated model is that the non-Markovian statistics of tracer trajectories arriving at $(t, \boldsymbol{x})$ from neighboring points $\boldsymbol{x}+\Delta\boldsymbol{x}$ and from past times $t-\Delta t$ become Markovian, Eulerian statistics at $(t, \boldsymbol{x})$ (Jeffery, 2000). As a result, each of the tracer particles in such a flow undergoes an effective Brownian motion and the first- and second-order moments of the passive scalar field (ignoring source terms) obey diffusion equations. The diffusion equation for the second-order correlation function $\Phi(\boldsymbol{r})$ assuming an incompressible and homogeneous velocity field is (Jeffery, 2000)

$$\frac{\partial \Phi}{\partial t} = 2D\Delta\Phi - 2\left[D_{mn}(0) - D_{mn}(\boldsymbol{r})\right]\frac{\partial^2 \Phi}{\partial x_m \partial y_n} + I, \tag{1}$$

where I is the contribution from source terms, $\boldsymbol{r}=\boldsymbol{y}-\boldsymbol{x}$, $D_{mn}(\boldsymbol{r})=\langle \tau u_m(0)u_n(\boldsymbol{r})\rangle$ with particle velocity component u_m and decorrelation time τ, and D is the molecular diffusivity. Note that summation is implied by repeated Roman indices.

Some remarks concerning the magnitude of D are in order. The diffusion of atmospheric cloud droplets due to Brownian motion is vanishingly small. However, at scales on the order of the droplet diameter, neighboring droplets can interact without collision if the ratio of their terminal velocities is in the range 2/3 to 3/2 (Pinsky et al., 2000). This interaction constitutes an effective Brownian motion with diffusivity $D \sim d^2\tau_\eta^{-1}$, where d is the droplet diameter and τ_η is the Kolmogorov time (Jeffery, 2000). Thus, for atmospheric cloud droplets where $d \approx 1$ μm and $\tau_\eta \approx 0.1$ s, $D=\mathcal{O}(10^{-11}$ m^2 s^{-1}) is small but finite.

Using isotropic and homogeneous viscous regime velocity correlation coefficients, Eq. (1) becomes (Jeffery, 2001a)

$$\frac{\partial \Phi}{\partial t} = 2D\Delta\Phi + \frac{|\gamma|}{3}\left[2r^2\delta_{mn} - r_m r_n\right]\frac{\partial^2 \Phi}{\partial r_m \partial r_n} + I, \tag{2}$$

where $\gamma \sim \tau_\eta$ is the average value of the least principal rate of strain. Eq. (2) describes a Brownian motion with effective diffusivity, $D_{\rm eff} \sim \tau_\eta r^2$, which can be compared with the inertial–convective (IC) result, $D_{\rm eff} \sim \varepsilon^{1/3} r^{4/3}$, first found empirically by Richardson (1926), where ε is the energy dissipation rate. The viscous–convective (VC) regime particle-pair separation described by Eq. (2) has important implications for the Shaw model of droplet spectral broadening (see Section 6). Given an initial particle separation $\rho^2(t=0)=\rho_0^2$, where ρ^2 is the mean-square particle separation averaged over the velocity field statistics, particles separate in the two regimes according to (Jeffery, 2001b):

- VC subrange: $\rho^2 = \rho_0^2 \exp(c_1 t/\tau_\eta)$
- IC subrange: $\rho^2 = \rho_0^2 + c_2 \varepsilon t^3$

where c_1 and c_2 are constants of order unity. In the IC subrange, ρ^2 becomes rapidly independent of the initial separation—particle trajectories have an inherent randomness analogous to the randomness of Brownian motion. This is not the case in the VC subrange where $\rho^2 \to 0$ as $\rho_0^2 \to 0$. However, the potential for a large ρ^2 after a small time t is greater in the VC regime where the particle separation is exponential.

Eq. (2) may be Fourier transformed to give

$$\frac{\partial \Psi}{\partial t} = -2Dk^2\Psi + \frac{|\gamma|}{3}\left[k^2\frac{\partial^2\Psi}{\partial k^2} + 4k\frac{\partial \Psi}{\partial k}\right] + I, \tag{3}$$

where Ψ is the spectral density. Eq. (3) with $I=0$ was first derived by Kraichnan (1968) who solved Eq. (3) with k greater than the Batchelor wave number and found k^{-1} scaling. Eqs. (2) and (3) are the starting points for the work presented in Jeffery (2000, 2001a).

3. Effect of particle inertia

In Jeffery (2000), the effect of particle inertia on the VC subrange is investigated. The study builds on the work of Elperin et al. (1996) who use the δ-correlated model to assess the effect of particle inertia on spatial statistics and have found a mechanism for intermittency in particle concentrations. They later present a solution for the correlation function of inertial particles at small scales (Elperin et al., 1998), i.e. the solution of a modified Eq. (2) that includes particle inertia. However, the results of Elperin et al. (1996, 1998) were not extended to spectral space and therefore the scales at which preferential concentration occurs were not ascertained.

The VC solutions presented in Elperin et al. (1998) and Jeffery (2000) were derived from Eq. (6) in Elperin et al. (1996), which, unfortunately, contains a sign error. This error was corrected in Jeffery (2001b) who found only superficial changes to the results in Jeffery (2000). The corrected results are summarized below.

Particles with small but finite inertia have velocity $\boldsymbol{u} \neq \boldsymbol{v}$ where $\boldsymbol{v}$ is the velocity of the surrounding fluid. Thus, in the case that $\boldsymbol{v}$ is divergenceless, homogeneous and isotropic, $\boldsymbol{u}$

is compressible, homogeneous and isotropic, and Eq. (1) with $I=0$ becomes (Jeffery, 2001b).

$$\frac{\partial\Phi}{\partial t} = 2D\Delta\Phi - 2\left[D_{mn}(0) - D_{mn}(\boldsymbol{r})\right]\frac{\partial^2\Phi}{\partial x_m\partial y_n} + 2\langle\tau b(\boldsymbol{x})b(\boldsymbol{y})\rangle\Phi$$
$$- 4\langle\tau u_m(\boldsymbol{x})b(\boldsymbol{y})\rangle\frac{\partial\Phi}{\partial y_m}, \tag{4}$$

where $b=\nabla\cdot\boldsymbol{u}$. Eq. (4) may be Fourier transformed and solved in the small $\boldsymbol{r}$ regime. The interested reader is referred to Jeffery (2000, 2001b) for further details. Here, only the final result is presented.

The spectral density Ψ of inertial particles at small scales is (Jeffery, 2001b)

$$\Psi = \begin{cases} C_1k^{\mu}K_{\mu}(\lambda_Bk) & k \geq k_m \\ C_3k^{2\mu}{}_2F_1(1/2-\mu,\ -\mu,\ 1-\mu;\ -Ak^{-2}) & k < k_m \end{cases} \tag{5}$$

valid for $\mu<0$ where ${}_2F_1$ is a hypergeometric function, K_μ is a modified Bessel function, $\mu=-3/2+5\sigma/(1+3\sigma)$, $A=10/11\eta^{-2}\sigma/(1+3\sigma)$, η is the Kolmogorov length, $C_3=\Gamma(-\mu)/2(\lambda_B/2)^{\mu}$, k_m is computed numerically from the intersection of the two functions, and λ_B is a diffusive length scale proportional to the Batchelor length. Here σ is a parameter that represents the degree of particle inertia via the compressibility of the particle's velocity according to $\sigma/(1+\sigma)=\tau_\eta^2\langle b^2\rangle$. Using a Gaussian expression for $\langle b^2\rangle$ from Pinsky et al. (1999) and assuming Stokes terminal velocity, Jeffery (2000) derived (see Section 5)

$$\frac{\sigma}{1+\sigma} = \tau_\eta^2\langle b^2\rangle = \frac{4}{15}St^2, \tag{6}$$

which relates σ to the Stokes number of the flow. Eq. (6) is generalized in Section 5 to incorporate non-Gaussian velocity statistics.

The scalar spectrum $E=4\pi k^2\Psi$, computed numerically using Eq. (5) and the inertial–convective range spectrum, is shown in Fig. 2, along with the change in scalar dissipation rate $\chi_{vc}(k)/\chi_{ic}$. The movement of the scale-break between the VC and IC regimes to smaller scales and the clumping of inertial particles with increasing St are clearly visible. Beginning at $St\approx0.2$ a peak at $k\approx0.1\eta^{-1}$ indicative of clumping is visible in the spectrum and becomes more pronounced as σ increases. Fig. 2 demonstrates that clumping begins near $St\approx0.2$ but is not significant until $St\geq0.3$. Although this finding supports the contention of Grabowski and Vaillancourt (1999) that cloud droplets ($St\leq0.07$ for $\varepsilon=10^{-2}$ m^2 s^{-3} and radius $r\leq15$ μm) are too small for significant preferential concentration to occur, we will see in Section 5 that velocity-gradient intermittency substantially increases $\langle b^2\rangle$ and hence σ at fixed St.

It should be emphasized that the criterion $St\geq0.3$ does not reflect the smallest St at which preferential concentration is statistically detectable. Rather, it is a measure of the smallest St at which the generation of small-scale covariance due to clumping at some scale k^{-1} becomes comparable in magnitude to the cascade of covariance from k^{-1} to

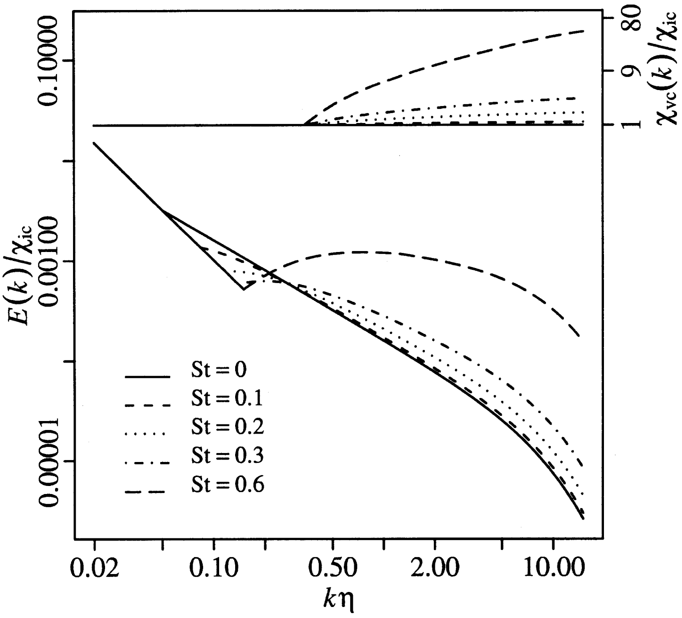

Fig. 2. The scalar spectrum computed at various St using Eqs. (5) and (6), and the corresponding increase in scalar dissipation rate. Particle clumping manifests as a bump in the spectrum which begins at $St \approx 0.2$ but does not become pronounced until $St \geq 0.3$. Parameter values are $\varepsilon = 0.01$ and Pr = 1000. Units are arbitrary.

smaller scales. Thus, for $St \geq 0.3$ small-scale generation of covariance dominates the usual cascade from large to small scales.

4. Effect of condensation and evaporation

In Jeffery (2001a), the study of the effect of condensation/evaporation on the viscous–convective subrange begins with the following stochastic equation for the cloud liquid water content q_l:

$$\frac{\partial q_l}{\partial t} + \boldsymbol{v}' \cdot \nabla q_l = D \Delta q_l + \frac{w'}{z} q_l \tag{7}$$

where z is the height above cloud base, w is the vertical velocity, a prime denotes mean-zero fluctuations and D is the molecular diffusivity. Ignoring molecular diffusion and assuming stationarity and horizontal homogeneity gives $\langle w' q_l' \rangle \sim z$, which agrees well with observational and numerical data. The source term $w' q_l / z$ is a mean-field approximation that decouples ql from the vapor and temperature fields. It is consistent with Lagrangian parcel models of diffusional growth of water drops in clouds where $\partial q_l / \partial t \sim (q_l / a) da/dt \sim q_l / t \sim w q_l / z$, and where a is the radius of the drop. The derivation of the source term is discussed in Jeffery (2001a) in more detail.

In Jeffery (2001a), I propose that the increased small-scale variability shown in Fig. 1 is caused by the effect of condensation and evaporation on the VC subrange. The condensation and evaporation source term of Eq. (7) is stochastic in w' and q_l, whereas for small scales, $r \ll z$, z is treated as a constant parameter. Closure of Eq. (7) using the δ-correlated model is considerably more complicated than the corresponding closure for inertial particles (Section 3) because fluctuations of q_l are non-homogeneous ($|q_l'|$ increases with increasing z) and axisymmetric. As a result, the spectral density is axisymmetric and complex.

Derivation of the spectral density Ψ proceeds as follows. First, the source term is neglected and the axisymmetric equivalent of Eq. (3) is derived:

$$\frac{\partial \Psi}{\partial t} = -2Dk^2\Psi + \frac{|\gamma|}{3}T(\Psi),$$

$$T(\Psi) = k^2\frac{\partial^2\Psi}{\partial k^2} + 4k\frac{\partial \Psi}{\partial k} + \frac{2\cos\theta}{\sin\theta}\frac{\partial \Psi}{\partial \theta} + 2\frac{\partial^2 \Psi}{\partial \theta^2}.$$

The solution can be written as a infinite series of Legendre polynomials in $\mu = \cos\theta$:

$$\Psi(k,\mu) = \sum_{j=0}^{\infty} c_j k^{-3/2} K_{v(j)}(\lambda_B k) P_j(\mu)$$

where $v(j) = [9 + 8j(j+1)]^{1/2}/2$, and where the Fourier space symmetry relation $\Psi(\boldsymbol{k}) = \Psi^*(-\boldsymbol{k})$ restricts the c_j's such that for even j, $Re\{c_j\} \in \mathbb{R}_+$ and $\mathrm{Im}\{c_j\} = 0$, whereas for odd j, $\mathrm{Re}\{c_j\} = 0$. Expansion of the scalar spectrum in terms of Legendre polynomials

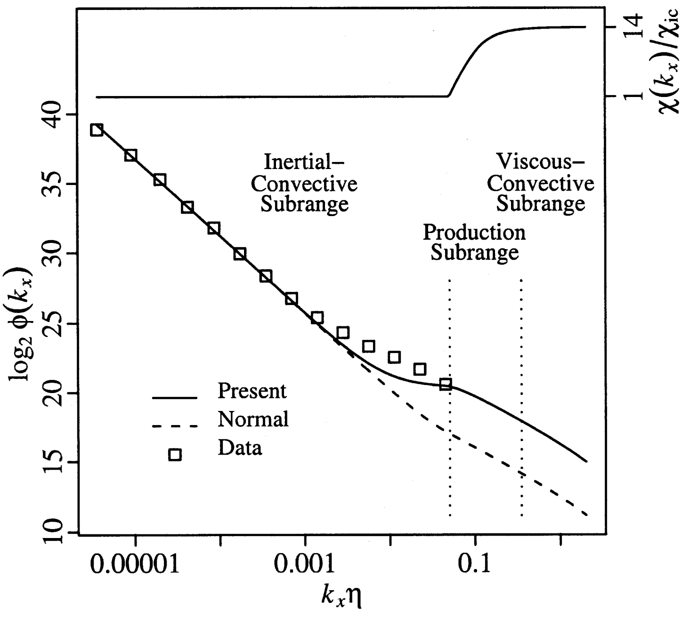

Fig. 3. Comparison of the ensemble-averaged 1D q_l scalar spectrum measured during SOCEX Davis et al. (1999) and the present model Eq. (8). A production subrange where $\chi(k_x)$ increases with increasing k (solid line), and normal VC scaling (dashed line) are also shown.

was first suggested by Herring (1974) who derived an equation for Ψ in axisymmetric turbulence using Kraichnan's direct interaction approximation (DIA).

The next step, described in Section 5 of Jeffery (2001a), is to add the source term. After some work, the resulting equation for the scalar spectrum is

$$E(k) = \frac{\chi}{|\gamma|}k^{-1}\left[1 + \lambda_B k\right]\exp(-\lambda_B k) - \frac{\chi}{|\gamma|}\frac{\zeta}{3}\lambda_B^{-2}k^{-3}, \tag{8}$$

where ζ is the "Kolmogorov constant" for the non-homogeneous (imaginary) component of the spectral density. The 1 D horizontal spectrum defined by $\phi(k_x) = \int_{k_x}^{\infty} k^{-1}\mathrm{d}kE(k)$ is shown in Fig. 3 along with the experimental data from Davis et al. (1999). Also shown is a "production subrange" where the scalar dissipation rate increases with increasing k. The good agreement between the modeled and observed spectra for $k \geq 0.02\eta^{-1}$ is not fortuitous—the unknown constant ζ was chosen to produce a close correspondence between the two spectra in this region. Fig. 3 reveals that the effect of condensation and evaporation as modeled by Eq. (7) can explain the anomalous scaling found by Davis et al. (1999).

5. *Re*$_\lambda$ dependence of *St*

In response to Grabowski and Vaillancourt's (1999) contention that the Stokes number of cloud droplets is too small for significant preferential concentration to occur, Shaw et al. (1999) argue that the Stokes number range for preferential concentration is significantly broader in clouds because of the large Reynolds number of atmospheric turbulence. More specifically, Shaw et al. (1999) point out that the fine-scale structure of large Reynolds number flow is highly intermittent (Sreenivasan and Antonia, 1997), and they suggest that small-scale coherent structures, i.e. vortex tubes, may influence the clumping process. Support for this claim comes from recent DNS experiments (Reade and Collins, 2000; Wang et al., 2000) that demonstrate an increase in the particle-pair radial distribution function with increasing Taylor micro-scale Reynolds number, Re_λ, at fixed St. Inspection of Eq. (4) reveals that the variance of the particle velocity flux divergence, $\langle b^2\rangle$, has the dominant and controlling Re_λ-dependence in the δ-correlated limit. Below, I estimate the effect of velocity field intermittency on $\langle b^2\rangle$.

Let $v_{i,j} \equiv \partial v_i/\partial x_j$ be the velocity gradient tensor of the surrounding fluid. Consider the symmetric strain tensor $s_{ij}=(v_{i,j}+v_{j,i})/2$ and the vorticity pseudovector $\omega_k = \epsilon_{kij}w_{ij}$ where the vorticity tensor $w_{ij}=(v_{i,j}-v_{j,i})/2$ and ϵ_{kij} is the alternating (Levi–Civita) symbol. Maxey (1987) first derived the relationship between the compressibility, $b = \nabla\cdot\boldsymbol{u}$, of an inertial particle's trajectory and the velocity, $\boldsymbol{v}$, of the surrounding fluid for $St < 1$:

$$\begin{aligned} b &= -\lambda^{-1}v_{i,j}v_{j,i} \\ &= -\lambda^{-1}(s^2 - \omega^2/2) \end{aligned} \tag{9}$$

where $\lambda = g/U_\mathrm{T}$, g is the acceleration of gravity and U_T is the magnitude of the particle's terminal fall velocity. Note this definition of λ differs by a factor of $(1-\rho_\mathrm{f}/\rho_\mathrm{p})^{-1}$ from the definition used in Pinsky et al. (1999) where ρ_f and ρ_p are the densities of the fluid and particle, respectively. This discrepancy can be traced back to the neglect of the fluid pressure in Khain and Pinsky (1995)'s Eq. (1).

Using Eq. (9), the zero–fourth-cumulant (Gaussian) hypothesis and assuming isotropy and incompressibility, Pinsky et al. (1999) derive

$$\langle b^2 \rangle = 60\lambda^{-2}\langle v_{1,1}^2 \rangle^2. \tag{10}$$

The St dependence for a particle falling at Stokes terminal velocity in a large Re_λ velocity field where $v_{1,1}^2 = \tau_\eta^{-2}/15$ is Jeffery (2000)

$$\langle b^2 \rangle = \frac{4}{15}\tau_\eta^{-2} St^2$$

in agreement with Eq. (6).

The Gaussian approximation used by Pinsky et al. (1999) to derive Eq. (10) is appropriate for fourth-order moments of the velocity field which are approximately Gaussian but it is unlikely to be accurate for fourth-order velocity gradients; large flows are highly intermittent. In fact, the flatness factor F of $v_{1,1}$ has a strong Re_λ dependence and reaches 20–25 in the atmospheric boundary-layer where $Re_\lambda = \mathcal{O}(10^4)$(Sreenivasan and Antonia, 1997, Fig. 6). This suggests that $\langle b^2 \rangle$ in the atmosphere may be a factor of 7–8 larger than the prediction of Eq. (10). On the other hand, $\langle v_{1,1}^4 \rangle$ is just one term in the expansion of $\langle b^2 \rangle$, and therefore, more information is required to determine the Re_λ-dependence of $\langle b^2 \rangle$.

Twenty years ago, Siggia (1981) demonstrated that fourth-order velocity derivative moments can be expressed as a linear combination of four irreducible scalar invariants: $I_1 = \langle s^4 \rangle$, $I_2 = \langle s^2\omega^2 \rangle$, $I_3 = \langle \omega_i s_{ij} s_{jk} \omega_k \rangle$ and $I_4 = \langle \omega^4 \rangle$, where $s^2 = \mathrm{tr}\mathbf{s}^2$. These four invariants are functions of familiar dynamical quantities (Pedlosky, 1987): $2\nu s^2$ is the kinetic energy dissipation rate, ω^2 is the enstrophy and $w_j s_{ij}$ is the vortex stretching term in the vorticity equation. Squaring Eq. (9) and substituting for I_α gives

$$\langle b^2 \rangle = \lambda^{-2}(I_1 - I_2 + I_4/4). \tag{11}$$

The Re_λ-dependence of $\langle b^2 \rangle$ follows from knowledge of I_1, I_2 and I_4. Furthermore, even if these three invariants have a simple power-law dependence on Re_λ, the resulting Re_λ-dependence of $\langle b^2 \rangle$ might be quite complex.

Unfortunately, measurement of I_α at large Reynolds numbers typical of the atmospheric boundary-layer has not yet been made. However, the task at hand simplifies if we assume that $\langle b^2 \rangle$ scales with $I_1 \sim \langle v_{1,1}^4 \rangle$. This approximation is justified at low Re_λ by the recent analysis of the ratios $A \equiv I_2/I_1$ and $C \equiv I_4/I_1$ by Zhou and Antonia (2000). Fig. 18 in Zhou and Antonia (2000) reveals that A and C have no discernible Re_λ-dependence for $Re_\lambda \leq 100$. We incorporate the Reynolds number dependence of preferential concentration into St by defining an effective Stokes number St_{eff}:

$$St_{\mathrm{eff}} = St(F/3)^{1/2}, \tag{12}$$

where $F \equiv \langle v_{1,1}^4 \rangle / \langle v_{1,1}^2 \rangle^2$ is the longitudinal flatness factor. Deviations of F above the Gaussian value of 3 are a manifestation of intermittency in the turbulence fine-scale structure.

In the atmospheric boundary-layer where $F \approx 22$, St_{eff} is around 2.7 St. Shaw et al. (1999, Table 1) estimate that $St \leq 0.02$ for kinetic energy dissipation rate $\varepsilon = 0.01$ m^2 s^{-3} and $St \leq 0.064$ for $\varepsilon = 0.1$ m^2 s^{-3} where $r \leq 8$ μm. Including the Re_λ dependence these numbers become $St_{\mathrm{eff}} \leq (0.054, 0.17)$, respectively. In Section 3, we found that clumping begins at $St \approx 0.2$ but does not become significant until $St \geq 0.3$. Thus for $r \leq 8$ μm, i.e. during most of a droplet's growth, is still too small for significant preferential concentration to occur. On the other hand, for larger drops with $r \geq 15$ μm, the Stokes number are $St_{\mathrm{eff}} \geq (0.19, 0.60)$, respectively. Thus, these large drops, particularly in high ε regions of a cloud, are preferentially concentrated.

The main assumption in the derivation of Eq. (12) is $I_1 \sim I_2 \sim I_4$, which has been verified for laboratory grid turbulence at $Re_\lambda \leq 100$. Obviously, this approximation should also be verified (or modified) from atmospheric data where $Re_\lambda = \mathcal{O}(10^4)$. Information on I_α and the 81 components of $\langle b^2 \rangle$ is given in Appendix A. Note that St_{eff}, which incorporates the increase in root-mean-square particle velocity divergence due to velocity field intermittency, may also be relevant in the parameterization of droplet-pair collision efficiencies. However, this application of St_{eff} is beyond the scope of the present investigation.

6. Vortex tubes and St_{eff}

At the heart of the arguments put forth by Shaw et al. (1998, 1999) is the requirement that the lifetime of a vortex tube increase with increasing Re_λ. For large Re_λ atmospheric flows, Shaw et al. (1998) choose a vortex lifetime τ_s of 5, 10, or 15 s. This value can be compared with the eddy turnover time $2\pi\tau_\eta \approx 0.26$ s. As pointed out by Grabowski and Vaillancourt (1999), the vortex in the Shaw model has to survive many tens of its turnover time to generate a strong effect on the cloud spectrum.

Long lifetimes, τ_s, are required to produce significant differences in the supersaturation between the droplet-depleted vortex and the droplet-rich environment. Further, the small number of droplets in the vortex must remain trapped for an eddy-trapping time $\tau_T \approx \tau_s$. Consequently, one would expect a small mean-square particle separation, $\rho^2(t)$, for $t = \tau_s$ in a vortex dominated field. However, in Section 2, we derived an exponential time-dependence for ρ^2 in the small-scale VC regime. This exponential time dependence implies that neighboring droplets rapidly reach inertial–convective regime separations, $\mathcal{O}(10\eta)$, where Richardson's law $\rho^2 \sim \varepsilon t^3$ holds. Moreover, increasing which enhances preferential concentration also increases $\rho^2(\tau_s)$ and, hence, decreases the supersaturation decorrelation time. An inverse relation between and the supersaturation decorrelation time was noted by Vaillancourt et al. (1998) in their numerical simulations (see also Vaillancourt and Yau, 2000). This behaviour is in contradistinction to the Shaw model where ρ^2 remains small for particles trapped in a vortex tube.

How can we reconcile the large ρ^2 predicted by the δ-correlated model with the large eddy-trapping times predicted by Shaw et al.'s (1998) vortex model? I believe that any contradictions are resolved by the following claim:

> Vortex tubes are not statistically relevant players in the dynamics of two-point passive scalar moments and/or pair separation at small-scales and large Re_λ.

Here, I present only a sketch of the argument which will be developed further in a forthcoming publication. Let us return to Eq. (11), which includes the effect of intermittency on particle clumping. Consider the following question: "How might the ratios $A \equiv I_2/I_1$ and $C \equiv I_4/I_1$ change in a velocity field dominated by cylindrical vortices?" Zhou and Antonia's (2000) experimental measurements indicate that while F increases from 3 to 4.5 as $Re_\lambda \to 100$, A and C remain constant near their Gaussian ratios of 1.43 and 4.76, respectively. The invariant I_2 is constrained by the incompressibility/homogeneity condition $\langle \omega^2 \rangle = 2\langle s^2 \rangle$. Thus, it is reasonable to expect I_2 and I_1 to scale with Re_λ such that A remains constant. On the other hand, there is no reason to expect the ratio C to remain near its Gaussian value in a velocity field dominated by cylindrical vortices which increase in intensity and persistence with increasing Re_λ.

In fact, a maximization of the ratio of the spatially averaged mean-square enstrophy to mean-square dissipation around a cylindrical vortex tube has been discussed by He et al. (1998). They find

$$C_{\mathrm{vort}} \approx 10.65,$$

spatially averaged over a single Burgers vortex and independent of the circulation which can be compared with the Gaussian value $C_{\mathrm{gauss}} \approx 4.76$. As a result, the increase in $\langle b^2 \rangle$ due to the presence of a Burgers vortex at fixed $I_1(Re_\lambda)$ is

$$\frac{1 - A + C_{\mathrm{vort}}/4}{1 - A + C_{\mathrm{gauss}}/4} \approx 2.9.$$

This analysis, albeit approximate, supports Shaw et al.'s (1998) claim that vortex tubes lead to increased particle clumping. On the other hand, Zhou and Antonia's (2000) experimental measurement of $C = 5 \pm 1$ does not support such a large value of C, albeit at $Re_\lambda \leq 100$. More to the point, their data does not indicate an increase in C with increasing Re_λ despite the increase in intensity and persistence of vortex tubes in this Re_λ regime. This brings us full circle to the comments of Grabowski and Vaillancourt (1999) who argue that the volume fraction of vortex tubes used by Shaw et al. (1998), 50%, is much too high. Grabowski and Vaillancourt (1999) suggest that 1% is more realistic. Indeed, Zhou and Antonia's (2000) measured value of $C = 5 \pm 1$ and a strong Re_λ dependence of I_1 is consistent with a relatively small volume fraction of vortex tubes superimposed on a highly non-Gaussian background velocity-gradient field. Thus, we conclude that it is the general intermittency of the velocity-gradient field as a whole, and not the presence of vortex tubes in particular, that could potentially lead to increased preferential concentration in atmospheric clouds.

7. $\boldsymbol{U}_{\mathrm{T}}$ and preferential concentration

Since Maxey and Corrsin (1986) first demonstrated an increase in droplet sedimentation velocity, $\boldsymbol{U}_{\mathrm{T}}$, resulting from the interaction of droplet inertia and turbulence, there has been a growing interest in the synergistic effects of inertia, sedimentation and turbulence on cloud microphysics. In particular, droplet coalescence rates are highly dependent on $\boldsymbol{U}_{\mathrm{T}}$. Recently, Vaillancourt et al. (1998) found a decrease in a 1-point measure of preferential concentration (the clustering index) with increasing $\boldsymbol{U}_{\mathrm{T}}$. In this section, I briefly discuss the effect of $\boldsymbol{U}_{\mathrm{T}}$ on preferential concentration.

Generalizing Maxey (1987)'s Eq. (5.13), we define the ballistic velocity, $\boldsymbol{u}_{\mathrm{T}}^{(p)}$, of the p-th moment of particle (droplet) number density, n, according to

$$\boldsymbol{u}_{\mathrm{T}}^{(p)}(\boldsymbol{v}) = \frac{\left\langle \int_{\Omega} n^{p}(\boldsymbol{x}) v(\boldsymbol{x}) d^{3}\boldsymbol{x} \right\rangle_{\boldsymbol{Y}}}{\left\langle \int_{\Omega} n^{p}(\boldsymbol{x}) d^{3}\boldsymbol{x} \right\rangle_{\boldsymbol{Y}}} \tag{13}$$

where $\boldsymbol{v}$ is the particle's velocity, Ω is a sample volume and $\langle \ldots \rangle_{\boldsymbol{Y}}$ represents a $\boldsymbol{v}$-dependent ensemble average over the subset of particle trajectories $\boldsymbol{Y}(t) \in \Omega$. Galilean invariance of n^{p} with respect to the still fluid sedimentation rate $\boldsymbol{U}_{\mathrm{T},0} = -U_{\mathrm{T},0}\hat{z}$ implies that $\boldsymbol{u}_{\mathrm{T}}^{(p)}(\boldsymbol{u} + \boldsymbol{U}_{\mathrm{T},0}) = \boldsymbol{U}_{\mathrm{T},0} + \boldsymbol{u}_{\mathrm{T}}^{(p)}(\boldsymbol{u})$ where u is the particle's velocity without sedimentation, i.e. $\boldsymbol{U}_{\mathrm{T},0}$ does not modify the statistics of n^{p}. Note that the usual $(p=1)$ droplet sedimentation velocity is defined according to $\boldsymbol{U}_{\mathrm{T}} = \boldsymbol{u}_{\mathrm{T}}^{(1)}(\boldsymbol{u} + \boldsymbol{U}_{\mathrm{T},0})$.

We first consider the effect of $\boldsymbol{U}_{\mathrm{T},0}$ on preferential concentration in the δ-correlated limit. Eq. (13) can easily be further generalized to describe the velocity of multi-point moments, e.g. the correlation function, Φ. Alternatively, the 2-point covariance sedimentation rate, $\boldsymbol{u}_{\mathrm{T}}^{(2)}$, in the δ-correlated limit is available directly from the advection term in Eq. (4) for $\partial\Phi/\partial t$:

$$\boldsymbol{u}_{\mathrm{T}}^{(2)}(\boldsymbol{v}) = \langle \boldsymbol{v} \rangle + 4\langle \tau \boldsymbol{v}(0) \nabla \cdot \boldsymbol{v}(\boldsymbol{r}) \rangle$$

where $\boldsymbol{r}$ is the separation between the two points. Immediately, we find that $\boldsymbol{u}_{\mathrm{T}}^{(2)}(\boldsymbol{u} + \boldsymbol{U}_{\mathrm{T},0}) = \boldsymbol{U}_{\mathrm{T},0} + \boldsymbol{u}_{\mathrm{T}}^{(2)}(u)$ provided that $\boldsymbol{u}$ is homogeneous; the advection of 2-point droplet number density fluctuations is Galilean invariant in the δ-correlated limit with respect to $\boldsymbol{U}_{\mathrm{T},0}$. It is easy to show that the diffusion term and source term in Eq. (4) are also Galilean invariant. How can we reconcile this with the numerical simulations of Vaillancourt et al. (1998), where the clustering index exhibits a $\boldsymbol{U}_{\mathrm{T},0}$-dependence? In fact, there is no inconsistency because the clustering index used by Vaillancourt et al. (1998) is a 1-point statistic involving clumping at all spatial scales according to $\Phi(0) = \int_{0}^{\infty} \mathrm{d}k E(k)$. The δ-correlated closure, on the other hand, holds true only in the small-scale VC regime of $E(k)$. Therefore, the $\boldsymbol{U}_{\mathrm{T},0}$-dependence of the clustering index is likely a manifestation of Lagrangian droplet–turbulence sedimentation interactions over scales greater than about 10η.

As noted above, $\boldsymbol{U}_{\mathrm{T}}$ plays an important role in many microphysical processes, particularly droplet coalescence. Maxey (1987, Eq.(5.18)) presents an approximate expression for $\boldsymbol{U}_{\mathrm{T}}$:

$$\boldsymbol{U}_{\mathrm{T}} = \boldsymbol{U}_{\mathrm{T},0} - \frac{1}{\Omega} \int_{\Omega} \int_{0}^{t} \langle \boldsymbol{u}(\boldsymbol{x}, t) b(\boldsymbol{Y}(t';\ \boldsymbol{x},\ t),\ t') \rangle \mathrm{d}t' d^{3}\boldsymbol{x}, \tag{14}$$

where $\boldsymbol{Y}(t';\boldsymbol{x},t) \in \Omega$ is the position at time t' of the particle that arrives at $(\boldsymbol{x},t)$. Assuming isotropy and taking the δ-correlated limit ($\mathrm{t} \to \tau$, $\boldsymbol{Y} \to \boldsymbol{x}$), we have $\boldsymbol{U}_{\mathrm{T}} \to \boldsymbol{U}_{\mathrm{T},0}$ as expected. This implies that VC subrange trajectories, $Y < \mathcal{O}(10\eta)$, do not contribute to $\boldsymbol{U}_{\mathrm{T}}$. Thus, it is the contribution from the relatively long inertial–convective regime particle paths $Y \geq \mathcal{O}(10\eta)$ that result in $U_T > U_{T,0}$ observed in numerical simulations (Wang and Maxey, 1993).

In Section 5, the Re_λ dependence of preferential concentration in the VC subrange was parameterized as a function of F. Determining the effect of velocity field intermittency on $\boldsymbol{U}_T$ is a much more difficult problem. Wang and Maxey (1993) argue that the presence of intense and persistent vortical structures will effect $\boldsymbol{U}_T$, which is suggestive of a strong Re_λ-dependence. On the other hand, relatively long temporal averaging that is characteristic of the large Y paths tends to dampen intermittency effects. The determination of the Re_λ dependence of $\boldsymbol{U}_T$ is surely one of the most challenging unsolved problems in cloud microphysics.

8. Summary

The small-scale variability of cloud liquid water is investigated using the δ-correlated closure. The spectral density of inertial particles in isotropic, homogeneous turbulence is derived in the small Stokes number regime ($St < 1$). In the scale range $13–60\eta$, a peak in the spectrum is observed when the ratio of the energies in the compressible and the incompressible components of the particle's velocity is greater than 0.01 ($St > 0.2$). The peak is a manifestation of preferential concentration—the accumulation of inertial particles in regions of high strain and low vorticity.

The effect of condensation and evaporation on the spectral density is also investigated using a simple mean-field model that reproduces the non-homogeneous vertical structure of liquid water fluctuations observed in atmospheric clouds. Expressions for the scalar density are derived and used to reproduce the spectral behaviour of new atmospheric measurements that exhibit anomalous scaling of cloud liquid water in the near inertial–convective regime. The model assumes a significant imaginary (non-homogeneous) component to the spectrum that is indicative of a strong vertical coherence in clouds. The strongly non-homogeneous (anisotropic) character of the predicted scalar spectrum is in stark contrast with atmospheric models of inertial–convective regime cloud inhomogeneity that are used in radiative transfer calculations and that are typically isotropic.

The debate over the existence of a preferential concentration of cloud droplets at small scales is fundamentally linked with the fine-scale structure of atmospheric turbulence. At the heart of the arguments put forth by Shaw et al. (1998, 1999) for a significant clumping of droplets is an explicit Reynolds number dependence of the relevant small-scale parameters. In particular, the lifetime of a vortex tube is assumed to increase linearly with Re_λ (Shaw et al., 1999, p. 1439). Although this time-scale is paramount for a Lagrangian analysis of individual droplet interactions with a single vortex tube, the relevant parameter in the Eulerian analysis of small-scale droplet number density is the variance of the scalar $v_{i,j}v_{j,i}$ averaged over both the vortex and background fields. This scalar variance is decomposed into three invariant contributions which, in turn, are explicit functions of symmetric strain and (antisymmetric) vorticity. Based on the recent experimental results of Zhou and Antonia (2000), an effective Stokes number is derived that is proportional to the square root of the flatness of the longitudinal velocity derivative, thereby explicitly incorporating the intermittency of the velocity field and an Re_λ-dependence into the theoretical framework developed using the δ-correlated closure. Using this effective Stokes number and an atmospheric flatness factor of 20–25, it is determined that intermittency may lead to appreciable clumping for large drops with radii greater than 15 μm under general atmospheric conditions. This finding supports the arguments made by Shaw et al. (1998, 1999) that intermittency enhances preferential concentration at small *St*.

On the other hand, the Shaw model of droplet spectral broadening is contingent on the interaction of cloud droplets and vortex tubes. Shaw et al. (1998, 1999) argue that the eddy-trapping time at large Re_λ is $\mathcal{O}(10\ \mathrm{s})$ which is approximately two orders of magnitude greater than the Kolmogorov time. Their arguments justifying such a large value are: (i) for a droplet trapped in a cylindrical vortex, the eddy-trapping time is equal to the vortex lifetime; (ii) vortex tubes are the (statistically) dominant small-scale feature at large Re_λ; (iii) vortex lifetimes may increase rapidly with increasing Re_λ. However, the suggestion of a statistically dominant role played by cylindrical vortices as Re_λ increases is inconsistent with experimental measurements which demonstrate that the ratio of mean-square enstrophy to mean-square dissipation is independent of Re_λ and close to the Gaussian value (Zhou and Antonia, 2000).

A huge increase in the eddy-trapping time resulting from the interaction of inertial droplets and vortex tubes is an essential component of the Shaw model of droplet spectral broadening, because spectral broadening does not occur if the droplets rapidly sample a range of supersaturations. Thus, in the absence of a dominant particle–vortex interaction, particle inertia could actually lead to spectral narrowing due to increased inertial mixing as pointed out by Pinsky and Khain (1997), Vaillancourt et al. (1998) and Pinsky et al. (1999).

Acknowledgements

I am grateful to Phillip Austin and Nicole Jeffery for a careful reading of the manuscript. I also thank Raymond Shaw and Katepalli Sreenivasan for helpful discussions during a 3-day workshop on fine-scale turbulence and cloud microphysics organized by NCAR's Geophysical Turbulence Program. In particular, I thank Sreenivasan for his interesting lecture on velocity field intermittency which motivated the development of St_{eff}.

Appendix A. $\langle b^2\rangle$–I_α Relations

Let $T_{\alpha\beta,\gamma\delta} = \langle v_{\alpha,\beta} v_{\beta,\alpha} v_{\gamma,\delta} v_{\delta,\gamma}\rangle$ where summation is not implied by repeated Greek indices. There are five non-trivial contributions to the 81 term in $\langle b^2\rangle$ if isotropy, homogeneity and incompressibility are assumed: $T_{\alpha\alpha,\alpha\alpha}$, $T_{\alpha\alpha,\alpha\beta}$, $T_{\alpha\alpha,\beta\gamma}$, $T_{\alpha\beta,\alpha\beta}$, $T_{\alpha\beta,\alpha\gamma}$. Note that $T_{\alpha\alpha,\beta\beta} =$

$T_{\alpha\alpha,\alpha\alpha}/2$. Following the procedure outlined in Siggia (1981), these five terms can be written in terms of the four invariants I_α:

$$T_{\alpha\alpha,\,\alpha\alpha} = \frac{4I_1}{105},$$

$$T_{\alpha\alpha,\,\alpha\beta} = \frac{I_1}{105} - \frac{I_2}{70} + \frac{I_3}{105},$$

$$T_{\alpha\alpha,\,\beta\gamma} = \frac{I_1}{105} - \frac{I_2}{210} - \frac{2I_3}{105},$$

$$T_{\alpha\beta,\,\alpha\beta} = \frac{3I_1}{140} - \frac{11I_2}{420} + \frac{I_3}{35} + \frac{I_4}{80},$$

$$T_{\alpha\beta,\,\alpha\gamma} = \frac{I_1}{140} - \frac{I_2}{84} - \frac{I_3}{70} + \frac{I_4}{240}.$$

The reader can easily verify that an enumeration of the contribution of these five terms to $\langle b^2 \rangle$ recovers Eq. (11). It may not always be possible to experimentally measure four of the above five terms independently. However, note that the relationship

$$\langle (v_{i,j}v_{j,i})^2 \rangle = 15T_{11,11} + 180T_{11,12} - 60T_{12,12} + 5\langle \omega_3^4 \rangle$$

may be particularly useful because it only involves three velocity gradients ($v_{1,1}$,$v_{1,2}$,$v_{2,1}$) and does not involve v_3 or $\hat{x}M_3 \equiv \hat{z}$. This may be advantageous if the measurements are made in a vertically sheared flow like the surface layer. The interested reader is referred to Siggia (1981) for further discussion on the experimental determination of I_α.

References

Cooper, W.A., Baumgardner, D., 1989. Comment on "the collection kernel for two falling cloud drops subjected to random perturbations in a turbulent air flow: a stochastic model". J. Atmos. Sci. 46 (8), 1165–1167.

Davis, A., Marshak, A., Gerber, H., Wiscombe, W.J., 1999. Horizontal structure of marine boundary-layer clouds from centimeter to kilometer scales. J. Geophys. Res. 104 (D6), 6123–6144.

Elperin, T., Kleeorin, N., Rogachevskii, I., 1996. Self-excitation of fluctuations of inertial particle concentration in turbulent fluid flow. Phys. Rev. Lett. 77 (27), 5373–5376.

Elperin, T., Kleeorin, N., Rogachevskii, I., 1998. Anomalous scalings for fluctuations of inertial particles concentration and large-scale dynamics. Phys. Rev. E 58 (3), 3113–3124.

Grabowski, W.W., Vaillancourt, P., 1999. Comments on "preferential concentration of cloud droplets by turbulence: effects on the early evolution of cumulus cloud droplet spectra". J. Atmos. Sci. 56, 1433–1441.

He, G., Chen, S., Kraichnan, R.H., Zhang, R., Zhou, Y., 1998. Statistics of dissipation and enstropy induced by localized vortices. Phys. Rev. Lett. 81 (21), 4636–4639.

Herring, J.R., 1974. Approach of axisymmetric turbulence to isotropy. Phys. Fluids 17 (5), 859–872.

Jeffery, C.A., 2000. Effect of particle inertia on the viscous–convective subrange. Phys. Rev. E 61 (6), 6578–6585.

Jeffery, C.A., 2001a. Effect of condensation and evaporation on the viscous–convective subrange. Phys. Fluids 13 (3), 713–722.

Jeffery, C.A., 2001b. Statistical models of cloud–turbulence interactions. PhD Thesis, Univ. British Columbia, Vancouver, Canada, September.

Khain, A.P., Pinsky, M.B., 1995. Drop inertia and its contribution to turbulent coalescence in convective clouds: Part I. Drop fall in the flow with random horizontal velocity. J. Atmos. Sci. 52 (2), 196–206.

Kraichnan, R.H., 1968. Small-scale structure of a scalar field convected by turbulence. Phys. Fluids 11 (5), 945–953.

Marshak, A., Davis, A., Wiscombe, W., Cahalan, R., 1998. Radiative effects of sub-mean free path liquid water variability observed in stratiform clouds. J. Geophys. Res. 103 (D16), 19557–19567.

Maxey, M.R., 1987. The gravitational settling of aerosol particles in homogeneous turbulence and random flow fields. J. Fluid Mech. 174, 441–465.

Maxey, M.R., Corrsin, S., 1986. Gravitational settling of aerosol particles in randomly oriented cellular flow fields. J. Atmos. Sci. 43 (11), 1112–1134.

Mazin, I., 1999. The effect of condensation and evaporation on turbulence in clouds. Atmos. Res. 51, 171–174.

Pedlosky, J., 1987. Geophysical fluid dynamics, 2nd edn. Springer-Verlag, New York.

Pinsky, M.B., Khain, A.P., 1997. Turbulence effects on droplet growth and size distribution in clouds—a review. J. Aerosol Sci. 28 (7), 1177–1214.

Pinsky, M.B., Khain, A.P., Levin, Z., 1999. The role of the inertia of cloud drops in the evolution of the spectra during drop growth by diffusion. Q. J. R. Meteorol. Soc. 125, 553–581.

Pinsky, M., Khain, A., Shapiro, M., 2000. Stochastic effects of cloud droplet hydrodynamic interaction in a turbulent flow. Atmos. Res. 53, 131–169.

Reade, W.C., Collins, L.R., 2000. Effect of preferential concentration on turbulent collision rates. Phys. Fluids 12 (10), 2530–2540.

Richardson, L.F., 1926. Atmospheric diffusion shown on a distance–neighbour graph. Proc. R. Soc. London, Ser. A 110, 709–737.

Shaw, R.A., Reade, W.C., Collins, L.R., Verlinde, J., 1998. Preferential concentration of cloud droplets by turbulence: effects on the early evolution of cumulus cloud droplet spectra. J. Atmos. Sci. 55, 1965–1976.

Shaw, R.A., Reade, W.C., Collins, L.R., Verlinde, J., 1999. Reply. J. Atmos. Sci 56, 1437–1441.

Siggia, E.D., 1981. In variants for the one-point vorticity and strain rate correlation functions. Phys. Fluids 24 (11), 1934–1936.

Sreenivasan, K.R., Antonia, R.A., 1997. The phenomenology of small-scale turbulence. Annu. Rev. Fluid Mech. 29, 435–472.

Tennekes, H., Woods, J.D., 1973. Coalescence in a weakly turbulent cloud. Q. J. R. Meteorol. Soc. 99, 758–763.

Vaillancourt, P.A., Yau, M.K., 2000. Review of particle–turbulence interactions and consequences for cloud physics. Bull. Am. Meteorol. Soc. 81 (2), 285–298.

Vaillancourt, P.A., Yau, M.K., Grabowski, W.W., 1998. Microscopic approach to cloud droplet growth by condensation. Conf. on Cloud Physics, Aug. Am. Meteorol. Soc., Everett, WA, pp. 546–549.

Wang, L.-P., Maxey, M.R., 1993. Settling velocity and concentration distribution of heavy particles in homogeneous isotropic turbulence. J. Fluid Mech. 256, 27–68.

Wang, L.-P., Wexler, A.S., Zhou, Y., 2000. Statistical mechanical description and modelling of turbulent collision of inertial particles. J. Fluid Mech. 415, 117–153.

Zhou, T., Antonia, R.A., 2000. Reynolds number dependence of the small-scale structure of grid turbulence. J. Fluid Mech. 406, 81–107.